Chemical Engineering Journal 441 (2022) 136077

Contents lists available at ScienceDirect

Chemical Engineering Journal

journal homepage: www.elsevier.com/locate/cej

Gradient trilayer solid-state electrolyte with excellent interface compatibility for high-voltage lithium batteries

Fang Liu [a,1], Yu Cheng [a,1], Xuri Zuo [a], Renpeng Chen [a], Jianyong Zhang [a], Liqiang Mai [a,b], Lin Xu [a,b,*]

[a] State Key Laboratory of Advanced Technology for Materials Synthesis and Processing, School of Materials Science and Engineering, Wuhan University of Technology, Wuhan 430070, PR China

[b] Foshan Xianhu Laboratory of the Advanced Energy Science and Technology Guangdong Laboratory, Xianhu Hydrogen Valley, Foshan 528200, Guangdong, PR China

ARTICLE INFO

Keywords:
Gradient
Trilayer
Interface
Solid-state electrolyte

ABSTRACT

Solid-state electrolytes (SSEs) are considered as promising alternatives for liquid electrolytes to achieve high energy density and safe lithium metal batteries. However, their practical utilization is limited owing to low ionic conductivity and insufficient interface stability. Here, a unique gradient trilayer SSE (20 μm) is designed to improve compatibility of anode/electrolyte/cathode interfaces and enhance structural integration to provide continuous Li^+ transport channels. One side anti-oxidation polymer layer improves the high-voltage tolerance for electrolyte/cathode interface, and the other side anti-reduction polymer layer provides soft interfacial contact and compatibility with Li-metal anode. Remarkably, the ultrathin porous membrane as host allows the fully penetration of two different polymers to form a gradient middle layer, providing excellent structural integration and fast Li^+ transport. Thus, the Li||Li symmetric cells with gradient trilayer electrolyte can stably operate over 2500 h under 0.1 mA cm^{-2}. The $LiNi_{0.8}Co_{0.1}Mn_{0.1}O_2$||Li solid-state batteries with gradient trilayer electrolyte deliver over 107 mAh g^{-1} capacity after 1000 cycles at 0.5C. This work provides a novel strategy to significantly enhance multilayer SSE with gradient interface in solid-state lithium-metal batteries.

1. Introduction

Solid-state lithium metal batteries (SSLMBs) with high-voltage cathode are expected to satisfy high energy density and more stringent safety requirements [1–4]. The development of solid electrolyte is one of the most critical steps of SSLMBs [5,6]. Unfortunately, no single solid electrolyte system can process excellent interfacial compatibility with both the Li-metal anodes and high-voltage cathodes concurrently to meet the demand for high energy density [7,8]. As the most extensively studied inorganic solid electrolytes, garnet $Li_7La_3Zr_2O_{12}$ (LLZO) shows high conductivity (10^{-4} S cm^{-1}) and electrochemical stability [9,10]. However, some drawbacks such as brittle nature and inadequate interfacial contact with electrodes result in the inorganic solid electrolytes displaying poor battery performance [11]. Among solid polymer electrolytes, The polyethylene oxide (PEO) solid electrolyte displays good interface compatibility with Li-metal anode [12]. However, it shows low ionic conductivity and poor mechanical strength [13,14]. Meanwhile, the PEO electrolyte is easily decomposed by $LiNi_xCo_yMn_zO_2$ (X + Y + Z = 1,0.5 < X < 1)(NCM) cathodes, which limits its application in high voltage cathode systems [15,16]. The polyvinylidene fluoride-co-hexafluoropropylene (PVDF-HFP) polymer has been widely used as solid state electrolyte because of their excellent antioxidative abilities, good film-forming properties, and high ionic conductivity, which makes it possible to match with high voltage cathode materials [13,17]. However, the rigid PVDF-HFP electrolyte shows poor physical contact with lithium metal, and even displays side reactions between the electrolyte and lithium metal [18,19]. Even though the composite solid electrolytes containing polymer and inorganic fillers become an innovative method to promote ionic conductivity and mechanical robustness, the electrolytes/electrodes interface problems have not been solved in a targeted manner [20,21]. To date, single solid electrolyte system has been caught in a dilemma to simultaneously meet the demands of high voltage tolerance and good lithium metal compatibility, high ionic conductivity, and good mechanical flexibility and strength [22–24].

To solve the aforementioned challenges, an intelligent strategy of

* Corresponding author.
E-mail address: linxu@whut.edu.cn (L. Xu).
[1] These authors contributed equally to this work.

https://doi.org/10.1016/j.cej.2022.136077
Received 31 January 2022; Received in revised form 24 March 2022; Accepted 26 March 2022
Available online 29 March 2022

designing multilayer electrolyte structure has attracted extensive attention [22,24–26]. Different functional solid electrolytes are applied and conformed to a composite matrix to solve the interfacial issues of cathode and anode, respectively [25,27,28]. Zhou et al. reported a double-layer polymer solid electrolyte (DLPSE) with a thickness of 240–260 μm, in which one polymer provides the interface stability of electrolyte/Li-anode, while the other side provides the compatibility with high-voltage cathode [29]. Another multilayered solid electrolyte was designed by stacking the oxidation-resistance poly(acrylonitrile) (PAN), the PAN@$Li_{1.4}Al_{0.4}Ge_{1.6}(PO_4)_3$ layer, and the reduction-resistant polyethylene glycol diacrylate (PEGDA) together, which delivers good interface compatibility in electrolytes/electrodes [30]. The different interface problems from the cathode and anode can be successfully solved by the multilayer structure, while the uncontrollable thickness of multilayer electrolytes and the lack of structural integration in this multilayer structure will lead to new interface problems. It still needs to be further ameliorated to obtain a better-integrated SSE [31–33].

Herein, we designed a gradient trilayer solid-state electrolyte (GTSSE) with excellent interface compatibility for high-voltage solid-state lithium metal batteries by a facile secondary casting and one-step drying process. In this GTSSE, the oxidation tolerant PVDF-HFP polymer can improve the interface high-voltage stability and form an indispensably continuous contact with cathode materials. On the anode side, the PEGDME polymer provides soft interfacial contact and remarkable compatibility with lithium metal anode. Meanwhile, the high porosity of ultrathin membrane not only improves mechanical properties as the firm host, but also allows the fully mobile and mutual penetration of two polymers aforementioned, working as gradient middle layer with fast Li^+ transport. This gradient layer evenly connects with other two heterogeneous polymer layers to remove new heterogeneous interface and enhance the integration of this trilayer structure, thus delivering continuous and uniform Li^+ transport channels. Moreover, the thickness of GTSSE is no more than 20 μm, thus reducing Li^+ transport distance and achieving better electrochemical performance, also improving the gravimetric/volumetric energy density. Because of the ingenious design, the as-obtained electrolyte provides short and continuous Li^+ transport paths, sufficient mechanical strength and excellent interface compatibility, demonstrated remarkable long-cycling performance in solid-state lithium-metal batteries derived from both $LiFePO_4$ (LFP) and $LiNi_{0.8}Co_{0.1}Mn_{0.1}O_2$ (NCM811). Remarkably, the NCM811|GTSSE|Li battery presents a reasonable discharge specific capacity of 107.1 mAh g^{-1} after an ultralong life of 1000 cycles.

2. Results and discussion

The schematic illustration for preparation process of a gradient trilayer solid electrolyte is seen in Fig. 1a. First, the PVDF-HFP-Li salt slurry is evenly coated on the glass plate with a scraper. Then the ultrathin porous membrane is laid flat on the PVDF-HFP slurry, and the slurry gradually penetrates into the pores of ultrathin membrane (Fig. S3, Fig. S4). When the ultrathin porous membrane is half soaked by PVDF-HFP, the PEGDME-Li salt slurry is uniformly dropped on the surface of the ultrathin porous membrane to fill the remaining space, in which 10 wt%PEO is added to improve the film-forming stability of PEGDME layer. PVDF-HFP and PEGDME will gradually mix inside the ultrathin porous membrane, and finally form continuous and gradient distribution as a gradient middle layer. The composite solid electrolyte is dried in the vacuum oven at 80 °C for 24 h to evaporate the dimethylformamide (DMF) solution. The as-obtained GTSSE with an ultrathin thickness of 20 μm exhibits fantastic mechanical flexibility (Fig. S1). In the solid-state battery (Fig. 1b), the GTSSE is constructed by an ultrathin porous membrane as the gradient layer to connect with other two functional layers. The high porosity ultrathin membrane as the host allows the fully mobile and mutual penetration of two polymer layers aforementioned, in which the blending polymer leads to a gradient middle layer, providing exceptional integration and ultrathin thickness. Furthermore, on the Li metal side, the PEGDME with more stable –OCH_3 group displays superior features in the interface compatibility with lithium-metal anode, which will form a favorable passivating solid-electrolyte interface (SEI) layer [3]. On the cathode side, considering that EO-based electrolyte is vulnerable when working in high voltage cathodes [17]. The PVDF-HFP with VDF-based polymer is designed to directly contact the cathode, which broadens the electrochemical window, as well as contributes to continuous contact among electrolytes and cathode with PVDF-HFP additives. The cross-sectional scanning electron microscopy (SEM) image of GTSSE is presented in Fig. 1c. The middle ultrathin porous membrane is evidently covered by these two polymers. Since the high porosity of ultrathin membrane allows the fully mobile and mutual penetration of two polymers aforementioned. Although the trilayer structure possesses obvious boundaries, which come from the edges of ultrathin porous membrane, the whole polymer component shows continuous distribution to ensure the structural integration. Moreover, the composite middle layer exhibits different polymer crystalline states between that of PVDF-HFP and PEGDME, proving the mixture of these two polymer contents, which will work as the gradient middle layer to eliminate the influence of

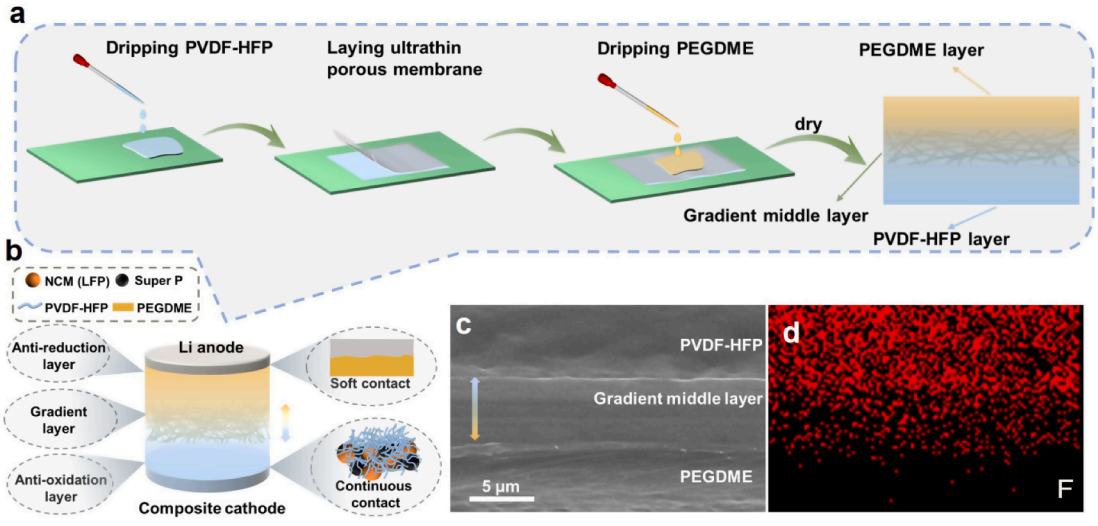

Fig. 1. Design and synthesis of gradient trilayer solid-state electrolyte. a) The diagram of preparation process for GTSSE. b) Structural schematic diagram of high-voltage lithium metal battery with GTSSE. c) Cross-sectional SEM image of the GTSSE. d) Cross-sectional EDS maps of GTSSE.

heterogeneous interface between different polymers in the trilayer electrolyte. The top side is fully covered with PVDF-HFP (Fig. S2a), and the oxidation tolerant polymer layer is beneficial to interface stability and continuous contact with composite cathode. The bottom side is covered by PEGDME (Fig. S2b), which can provide excellent interface compatibility and soft interfacial contact with Li anode. From the section–view of Fig. 1d, the EDS mapping reveals that the F element is inhomogeneously distributed in this trilayer structure. According to the concentration of F element in the middle layer, different from that in the PVDF-HFP layer, it shows a decreasing trend from the PVDF-HFP side to the PEGDME side, proving that the gradient polymer distribution is successfully constructed.

The X-ray diffraction (XRD) in Fig. 2a is used to examine and characterize the crystallinity of GTSSE, PVDF-HFP membrane and PEGDME membrane. Compared with the characteristic peaks of PVDF-HFP membrane and PEGDME membrane, the characteristic peaks of GTSSE are weaker, showing the preliminary mixture of these two polymers in the mixture. However, GTSSE shows higher crystallinity than PVDF-HFP/PEGDME mixed membrane, suggesting that the mixture of two polymers occurs in the middle layer. On the two sides of this mixing region, the pure PVDF-HFP and PEGDME layers are still remained. This inhomogeneous distribution will be helpful for the construction of the middle gradient layer with low crystallinity region [34,35]. Electrochemical impedance spectroscopy (EIS) measurement was carried out by using stainless steel|SSEs|stainless steel symmetric cells for ionic conductivity of SSEs ranging from 20 °C to 60 °C in Fig. 2b. The GTSSE presents the ionic conductivity of 2.91×10^{-5} S cm^{-1} and 1.32×10^{-4} S cm^{-1} at 20 °C and 50 °C, respectively, higher than those of the PVDF-HFP electrolyte (1.58×10^{-5} S cm^{-1} at 20 °C and 9.12×10^{-5} S cm^{-1} at 50 °C) and the PEGDME electrolyte (1.07×10^{-5} S cm^{-1} at 20 °C and 8.58×10^{-5} S cm^{-1} at 50 °C) (Fig. S5a, b). The ionic conduction of the GTSSE is obviously enhanced, which can be attributed to the gradient middle layer with fast lithium-ion transport. Meanwhile, the ionic conductivity at different temperatures can be fitted by the Vogel–Fulcher–Tamman equation (Fig. 2c). Because of the synergistic effect of electrolyte structure integrity and fast lithium-ion transport layer inside gradient middle layer, the energy barrier becomes lower for Li^+ transport in GTSSE. Therefore, the fitting value of activation energy (Ea) for GTSSE electrolyte is 0.393 eV, which is noticeably lower than that for PVDF-HFP electrolyte (0.457 eV) and PEGDME electrolyte (0.538 eV). The lithium-ion transference number (t_{Li^+}) is another key factor for proper function in battery systems. For symmetric Li|GTSSE|Li cell, a relatively high (0.38, Fig. 2d) is acquired at room temperature (RT), which is close to the theoretical maximum value of most polymer electrolyte (=0.4) [36]. Moreover, the above-mentioned exceptional electrochemical performances of GTSSE also take advantage of its lower glass transition temperature (Fig. S6), which is more favorable for the rapid transfer of lithium ions [37,38].

The electrochemical window is a dominant parameter of the electrolyte applicability for high-voltage Li metal batteries. As presented in Fig. 2e, the PEGDME electrolyte began to decompose at 4.2 V (versus Li^+/Li), while the GTSSE can be stable up to 4.8 V due to the combination of PVDF-HFP layer, indicating the GTSSE design can be combined with high-voltage cathodes. Thermal stability of PVDF-HFP electrolyte, PEGDME electrolyte, and GTSSE was evaluated by thermogravimetric analysis (TGA). The GTSSE started to decompose at a relatively high temperature over 240 ℃, indicating the DMF solvent has been completely removed, as well as the GTSSE has good thermal stability compared with PVDF-HFP electrolyte and PEGDME electrolyte (Fig. S7). In Fig. 2f, the GTSSE displays a high modulus of 9.59 MPa, which is clearly higher than that of PVDF-HFP membrane (2.51 MPa) and PEGDME membrane (0.18 MPa). The stress–strain tests verify that the GTSSE has sufficient mechanical strength while ensuring short lithium-ion transport distance properties due to the introduction of the ultrathin porous membrane as a host.

The interfacial performance for long-term cycling stability and voltage polarization of Li|SSEs|Li symmetric cell was investigated by long-term lithium stripping/plating experiment at 0.1 mA cm^{-2} for the area capacity of 0.1 mAh cm^{-2} (in Fig. 3a). To avoid direct contact between PVDF-HFP and lithium metal, another PEGDME layer was covered on the PVDF-HFP side to form Li|PEGDME|GTSSE|Li cell (Fig. S8). As shown in Fig. 3a, the Li|PEGDME|GTSSE|Li cell exhibits outstanding electrochemical stability, and the initial polarization voltage value cycling is 25 mV, and after cycling for 2500 h is 48 mV. Conversely, the Li|PVDF-HFP|Li cell shows a rapid and continuously increasing polarization voltage and finally the battery broke down after only 192 h of cycling, which indicates inferior interfacial stability owing to the adverse reactions between PVDF-HFP and Li metal. Unlike the

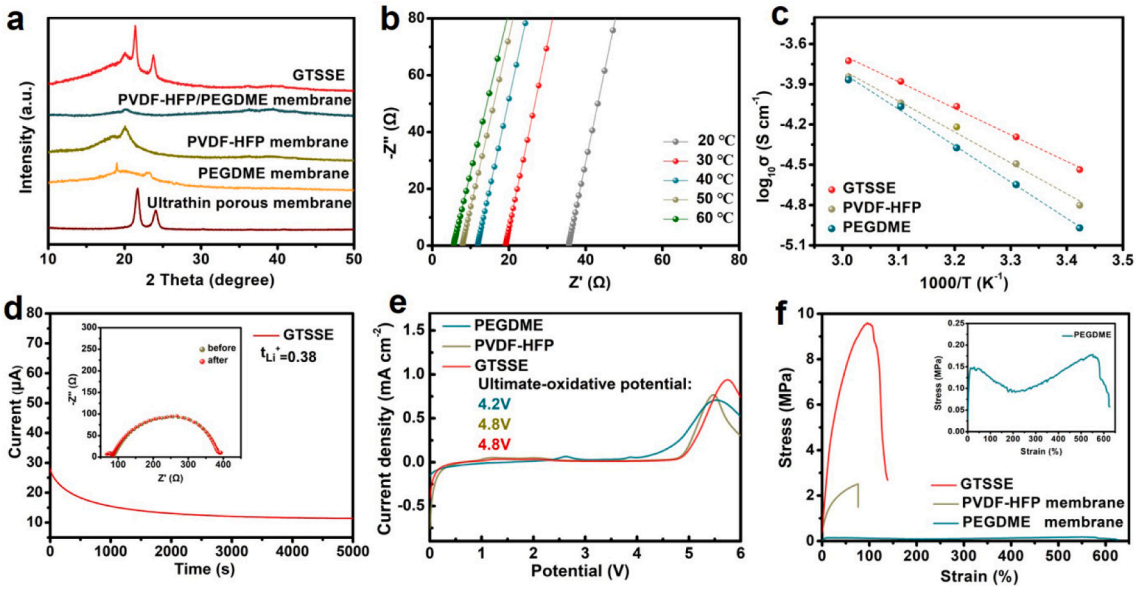

Fig. 2. Characterizations of gradient trilayer solid-state electrolyte a) XRD patterns of ultrathin porous membrane, PVDF-HFP membrane, PEGDME membrane, PVDF-HFP/PEGDME membrane, and GTSSE. b) EIS curves of GTSSE from 20 to 60 °C. c) Arrhenius plots of different SSEs. d) Current–time curve following DC polarization of Li|GTSSE|Li symmetrical cell at 10 mV s^{-1} (inset: EIS variation before and after polarization at RT). e) LSV curves of PVDF-HFP electrolyte, PEGDME electrolyte, and GTSSE at RT. f) Stress–strain curves of PVDF-HFP membrane, PEGDME membrane, and GTSSE (inset: PEGDME membrane curve was magnified).

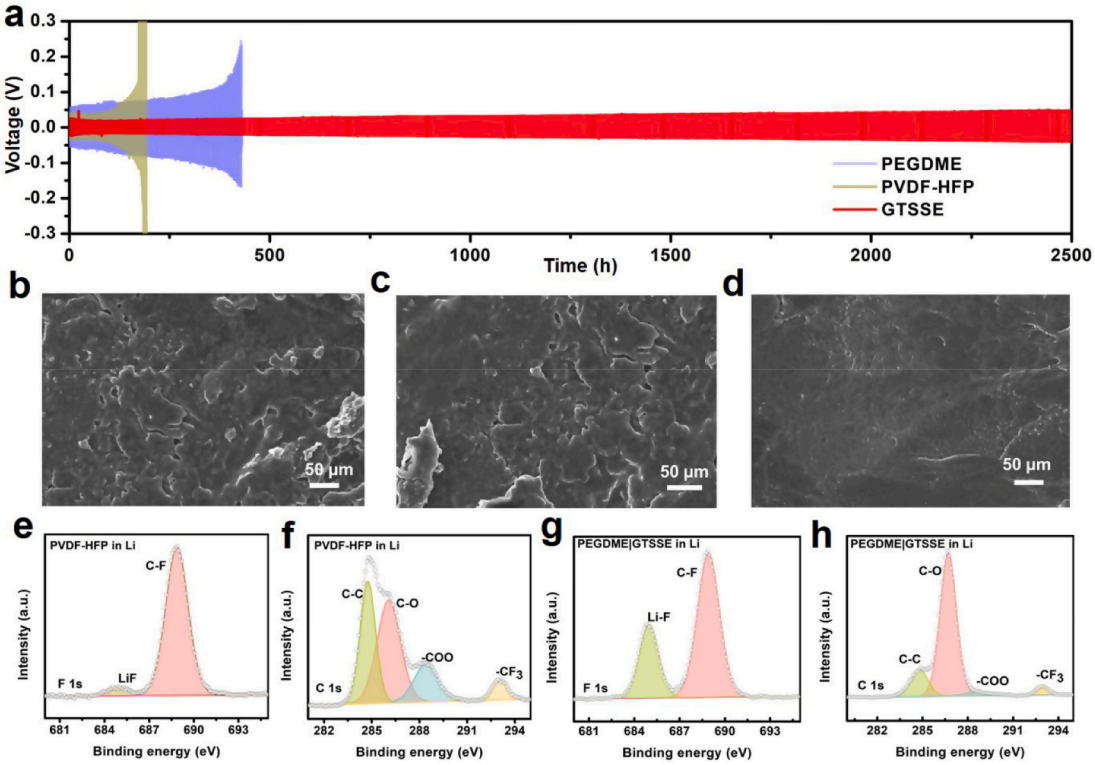

Fig. 3. Symmetric cells with gradient trilayer solid-state electrolyte. a) Galvanostatic cycling of the Li|PVDF-HFP|Li, Li|PEGDME|Li, and Li|GTSSE|Li symmetric cells at a current density of 0.1 mA cm^{-2} for 0.1 mAh cm^{-2}. Surface morphology images of Li metal b) in PVDF-HFP electrolyte, c) in PEGDME electrolyte, and d) in GTSSE after lithium plating/stripping 192 h, 432 h, and 2500 h, respectively. XPS spectra of Li anodes from e-f) Li|PVDF-HFP|Li and g-h) Li|PEGDME|GTSSE|Li symmetric cells after lithium plating/stripping 192 h and 2500 h, respectively.

PVDF-HFP electrolyte, the cells assembled with the PEGDME electrolyte last for 432 h without short circuit, implying good interface stability between the PEGDME layer and Li anodes. However, the Li|PEGDME|Li cell shows slightly increased polarization voltage due to the lower ionic conductivity of PEGDME electrolyte. This result indicates that the excellent long-cycle stability of the GTSSE is not only due to the good interfacial compatibility of PEGDME with Li metal, but also due to the low crystalline region of the gradient middle layer in the GTSSE which is beneficial to fast Li-ion transport, thus exhibiting low polarization. To explain the reasons behind the excellent performance in Li|GTSSE|Li cell, the surface morphologies of Li metal after cycling are presented via SEM images. The Li|PVDF-HFP|Li and Li|PEGDME|Li symmetric cells were cycled for 192 h and 432 h, respectively. Obviously, these cracks and pores are observed on the surface of Li metal (Fig. 3b, c). On the contrary, the Li|PEGDME|GTSSE|Li cell shows a flat lithium surface, although it looks like the surface has a few cracks without lithium dendrites growing after 2500 h cycling (Fig. 3d). The X-ray photoelectron spectroscopy (XPS) spectra of F 1 s and C 1 s of Li anodes after cycling are depicted in Fig. 3e-h. The C 1 s spectra contain four peaks characteristic of C–C, C-O, –COO, and -CF_3 bonds. For the GTSSE, the peaks of C–C, C-O, –COO are greatly reduced compared with PVDF-HFP electrolyte, revealing that the SEI layer is more stable and generated fewer side products [39]. Moreover, a strong LiF peak is detected from Li anode in the Li|PEGDME|GTSSE|Li cell, which promotes long-term uniform lithium plating/stripping behaviors [40–42].

In order to evaluate the practicality of three SSEs in SSLMBs, the LFP|SSEs|Li batteries were assembled and tested at 50 ℃. The long-term cycling performance of the LFP|GTSSE|Li battery is much better than that of the LFP|PEGDME|Li and LFP|PVDF-HFP|Li batteries presented in Fig. S9a. The LFP|GTSSE|Li battery shows an initial discharge capacity of 142.5 mAh g^{-1} at 0.5C and displays a slight and negligible overpotential increase than control sample during long-term cycling (Fig. S9b; Fig. S10a, b,). The discharge capacity stabilizes 135.4 mAh g^{-1} after 150 cycles, corresponding to 95% of the initial discharge capacity. By contrast, the LFP|PEGDME|Li and LFP|PVDF-HFP|Li batteries present a fast capacity decay and exhibit badly discharge capacity of 93.8 mAh g^{-1} (LFP|PEGDME|Li) and 27.3 mAh g^{-1} (LFP|PVDF-HFP|Li) after 150 cycles. These results show significantly improved capacity retention on account of the synergistic effect of the reliable interface stability and the gradient middle layer with fast Li^+ transport in GTSSE. Moreover, the rate performance of the LFP|SSEs|Li batteries under different rates from 0.1 to 1C are displayed in Fig. S9c, the discharge capacity curves of LFP|PEGDME|Li and LFP|PVDF-HFP|Li batteries decrease sharply and the gaps compared with LFP|GTSSE|Li are getting larger when the current density increases. Meanwhile, the discharge voltage plateau of the GTSSE battery slowly descends without serious polarization (Fig. S11). Especially at 1C, the LFP|PEGDM|Li and LFP|PVDF-HFP|Li batteries only deliver 87.7 mAh g^{-1} and 12.5 mAh g^{-1}, respectively, while the LFP|GTSSE|Li batteries can still possess an excellent discharge capacity of 126.3 mAh g^{-1}.

To demonstrate the ability of SSEs operating at higher voltage, the NCM811|SSEs|Li batteries were assembled for further study. As shown in Fig. 4a, the NCM811|SSEs|Li batteries were activated at a small current (0.1C, 1st-3rd). The galvanostatic charge–discharge curves of NCM811|PVDF-HFP|Li or NCM811|PEGDME|Li delivery sudden capacity fade and even cannot work 200 cycles at 0.5C at 50 °C. In sharp contrast, the NCM811|GTSSE|Li battery demonstrates a high discharge capacity retention of 83% (137 mAh g^{-1}) of the initial capacity (4th:164.7 mAh g^{-1}) after 200 cycles. Moreover, the NCM811|GTSSE|Li battery still presents a reasonable cyclability discharge specific capacity of 107 mAh g^{-1} after an ultralong cycle life of 1000 cycles at 0.5C. It is demonstrated that the ultrathin gradient trilayer SSE with no other

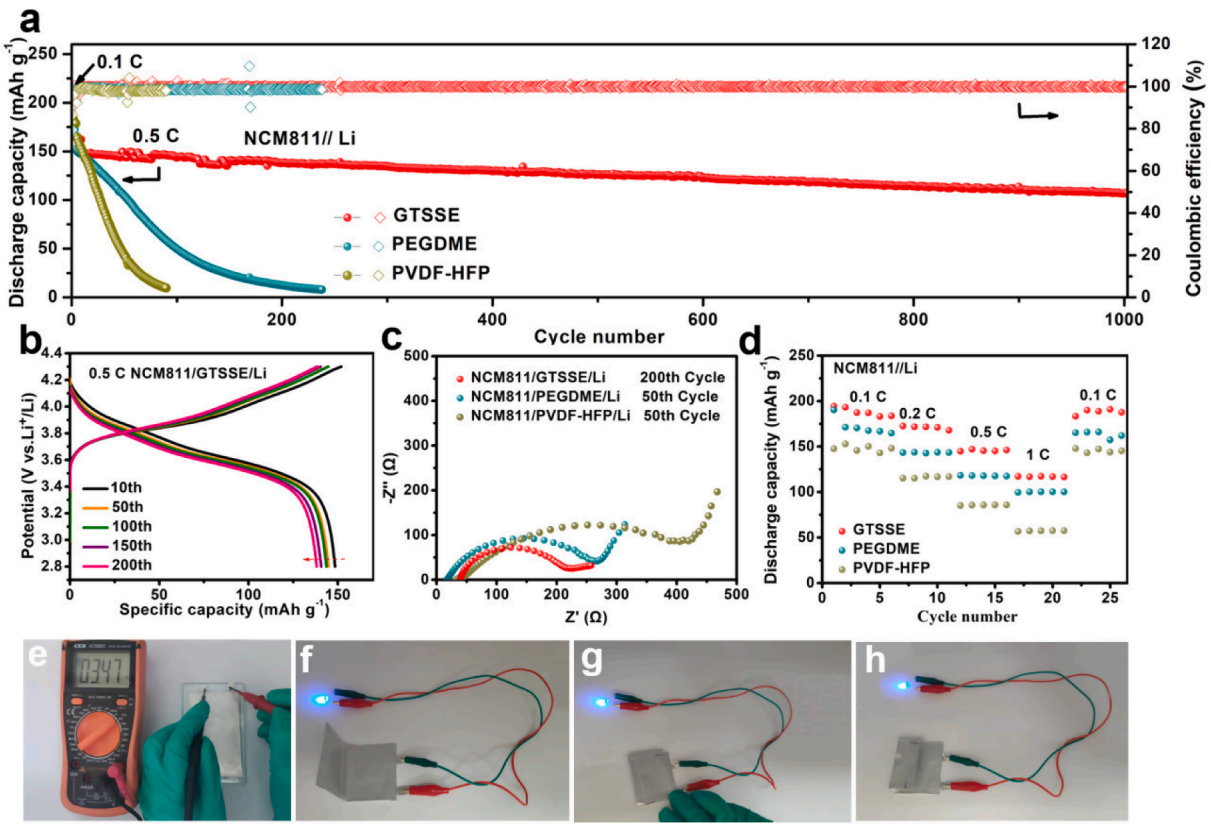

Fig. 4. NCM811||Li full batteries with gradient trilayer solid-state electrolyte. a) Cycling performance of NCM811||Li batteries with different SSEs at 0.5C, together with the typical voltage profiles of b) the GTSSE. c) Nyquist plots of the LFP|PVDF-HFP|Li, LFP|PEGDME|Li batteries after 50 cycles, and LFP|GTSSE|Li batteries after 200 cycles. d) Rate performances of NCM811||Li batteries with SSEs. e) The voltage images of the NCM811|GTSSE|Li battery under original. f-h) Optical photographs of the flexible NCM811|GTSSE|Li pouch battery can light up LED lamps under different conditions.

heterogeneous interface not only effectively improves long-term interface stability between SSE and high-voltage NCM811 cathode materials, but also enhances structural integration to provide continuous and uniform Li^+ transport channels. As shown in Fig. 4b, the NCM811|GTSSE|Li battery shows a significantly lower overpotential increase than that of NCM811|PVDF-HFP|Li battery and NCM811|PEGDME|Li battery (Fig. S12a, b). The reason for this result is that in the GTSSE one side anti-oxidation polymer (PVDF-HFP) layer improves the high-voltage tolerance and continuous contact for electrolyte/cathode interface, and the other side anti-reduction polymer (PEGDME) layer provides soft interfacial contact and compatibility with Li-metal anode. Meanwhile, the GTSSE with a gradient middle layer, provides excellent structural integration and fast Li^+ transport channels. The lower polarization voltage observed in typical charge/discharge profiles indicates slight polarization, which is favorable for long-term cycling. The charge transfer resistance (R_{ct}) and the interface resistance (R_{if}) are represented in the middle frequency region [43–45]. The resistances (R_{ct} + R_{if}) of NCM|PVDF-HFP|Li, NCM|PEGDME|Li and NCM811|GTSSE|Li batteries before cycling are 198.0 Ω, 176.3 Ω and 151.0 Ω, respectively (Fig. S13). Whereas, the resistance of NCM811|PVDF-HFP|Li (438.4 Ω) and NCM811|PEGDME|Li (281.6 Ω) greatly increases after 50 cycles, the NCM811|GTSSE|Li battery still remains a relatively stable interfacial resistance (219.8 Ω) (Fig. 4c), indicating that the GTSSE can effectively help to improve the interfacial stability between the electrolyte and electrodes.

Fig. 4d and Fig. S14 show the rate performance of the NCM811|SSEs|Li batteries. The NCM811|GTSSE|Li battery shows discharge capacities of 188, 172, 165, 145, and 117 mAh g^{-1} at 0.1, 0.2, 0.5, and 1C, respectively, and also delivers superior capacity reversibility when current density backs to 0.1C (187 mAh g^{-1}), illustrating that the electrolyte hardly decompose at high current density and the interfaces between electrolyte and electrodes are still in stable adhesion. On the contrary, the batteries using PEGDME or PVDF-HFP electrolytes show low discharge capacity and obvious capacity decay with the increase of current density, which is mainly due to poor interface stability and low ionic conductivity. For practical evaluation, the NCM811|GTSSE|Li pouch batteries were assembled shown in Fig. 4e-h. The pouch battery shows an open circuit voltage of 3.7 V and could make the LED device work normally after curling to multiple folding, and even being cut twice (Fig. S15). Benefitting from the structural integration of the GTSSE, the polymer layers in the GTSSE will not fall off with multiple folding, and the pouch batteries show high safety after twice cutting.

3. Conclusion

In summary, we designed a gradient trilayer solid electrolyte (20 μm) with excellent interface compatibility for ultralong-life and high-voltage solid-state batteries by a facile secondary casting and one-step drying process. The GTSSE possesses two functional layers to provide interface compatibility with cathode and lithium metal anode, respectively. The gradient middle layer with ultrathin firm porous membrane and uniform polymer blending delivers enhanced structural integration and continuous Li^+ transport channels. The obtained GTSSE shows a high ionic conductivity of 1.32 × 10^{-4} S cm^{-1}at 50 ℃ and an electrochemical window of 4.8 V. As a result of the exceptional intrinsic advantages of the GTSSE, the Li|GTSSE|Li symmetric cell can stably plated/stripped for more than 2500 h at the current density of 0.1 mA cm^{-2}. The LFP|GTSSE|Li battery delivers highly capacity retention of 95% after 150

cycles at 0.5C. Notably, the NCM811|GTSSE|Li battery still presents a reasonable cycle ability discharge specific capacity of 107.1 mAh g^{-1} after an ultralong cycle life of 1000 cycles at 0.5C. The GTSSE provides a promising model based on gradient multilayer electrolyte structure to develop safe and high energy density solid-state Li metal batteries.

Declaration of Competing Interest

The authors declare that they have no known competing financial interests or personal relationships that could have appeared to influence the work reported in this paper.

Acknowledgements

F.L. and Y.C. contributed equally to this work. This work was supported by the National Key Research and Development Program of China (2020YFA0715000), the National Natural Science Foundation of China (51802239, 51832004), the Key Research and Development Program of Hubei Province (2021BAA070), Foshan Xianhu Laboratory of the Advanced Energy Science and Technology Guangdong Laboratory (XHT2020-005, XHT2020-003).

Appendix A. Supplementary data

Supplementary data to this article can be found online at https://doi.org/10.1016/j.cej.2022.136077.

References

[1] M. Li, C. Wang, Z. Chen, K. Xu, J. Lu, New concepts in electrolytes, Chem Rev. 120 (14) (2020) 6783–6819.
[2] X. Wang, R. Kerr, F.F. Chen, N. Goujon, J.M. Pringle, D. Mecerreyes, M. Forsyth, P. C. Howlett, Toward high-energy-density lithium metal batteries: opportunities and challenges for solid organic electrolytes, Adv. Mater. 32 (2020), e1905219.
[3] X.F. Yang, M. Jiang, X.J. Gao, D. Bao, Q. Sun, N. Holmes, H. Duan, S. Mukherjee, K. Adair, C. Zhao, J. Liang, W. Li, J. Li, Y. Liu, H. Huang, L. Zhang, S. Lu, Q. Lu, R. Li, C.V. Singh, X. Sun, Determining the limiting factor of the electrochemical stability window for PEO-based solid polymer electrolytes: main chain or terminal –OH group? Energy Environ. Sci. 13 (2020) 1318–1325.
[4] Y.L. Liu, Y. Zhao, W. Lu, L.Q. Sun, L. Lin, M. Zheng, X.L. Sun, H.M. Xie, PEO based polymer in plastic crystal electrolytes for room temperature high-voltage lithium metal batteries, Nano Energy 88 (2021), 106205.
[5] J. Wan, J. Xie, D.G. Mackanic, W. Burke, Z. Bao, Y. Cui, Status, promises, and challenges of nanocomposite solid-state electrolytes for safe and high performance lithium batteries, Mate. Today Nano 4 (2018) 1–16.
[6] Y. Cheng, J. Shu, L. Xu, Y.Y. Xia, L.L. Du, G. Zhang, L.Q. Mai, Flexible Nanowire Cathode Membrane with Gradient Interfaces and Rapid Electron/Ion Transport Channels for Solid-State Lithium Batteries, Adv. Energy Mater. 11 (2021) 2100026.
[7] Y. Chen, K.H. Wen, T.H. Chen, X.J. Zhang, M. Armand, S.M. Chen, Recent progress in all-solid-state lithium batteries: The emerging strategies for advanced electrolytes and their interfaces, Energy Storage Mater. 31 (2020) 401–433.
[8] L. Fan, S.Y. Wei, S.Y. Li, Q. Li, Y.Y. Lu, Recent Progress of the Solid-State Electrolytes for High-Energy Metal-Based Batteries, Adv. Energy Mate. 8 (2018) 1702657.
[9] B. Jiang, Y. Wei, J. Wu, H. Cheng, L. Yuan, Z. Li, H. Xu, Y. Huang, Recent progress of asymmetric solid-state electrolytes for lithium/sodium-metal batteries, Energy Chem. 3 (5) (2021) 100058.
[10] L.S. Li, Y.F. Deng, G.H. Chen, Status and prospect of garnet/polymer solid composite electrolytes for all-solid-state lithium batteries, J. Energy Chem. 50 (2020) 154–177.
[11] C.W. Sun, J. Liu, Y.D. Gong, D.P. Wilkinson, J.J. Zhang, Recent advances in all-solid-state rechargeable lithium batteries, Nano Energy 33 (2017) 363–386.
[12] J. Lu, Y. Liu, P.H. Yao, Z.Y. Ding, Q.M. Tang, J.W. Wu, Z.R. Ye, K. Huang, X.J. Liu, Hybridizing poly(vinylidene fluoride-co-hexafluoropropylene) with $Li_{6.5}La_3Zr_{1.5}Ta_{0.5}O_{12}$ as a lithium-ion electrolyte for solid state lithium metal batteries, Chem. Eng. J. 367 (2019) 230–238.
[13] H. Xu, H. Zhang, J. Ma, G. Xu, T. Dong, J. Chen, G. Cui, Overcoming the Challenges of 5 V Spinel $LiNi_{0.5}Mn_{1.5}O_4$ Cathodes with Solid Polymer Electrolytes, ACS Energy Lett. 4 (12) (2019) 2871–2886.
[14] W. Zhou, S. Wang, Y. Li, S. Xin, A. Manthiram, J.B. Goodenough, Plating a Dendrite-Free Lithium Anode with a Polymer/Ceramic/Polymer Sandwich Electrolyte, J. Am. Chem. Soc. 138 (30) (2016) 9385–9388.
[15] P. Ding, Z. Lin, X. Guo, L. Wu, Y. Wang, H. Guo, L. Li, H. Yu, Polymer electrolytes and interfaces in solid-state lithium metal batteries, Mater. Today 51 (2021) 449–474.
[16] L.P. Yue, J. Ma, J.J. Zhang, J.W. Zhao, S. Dong, Z.H. Liu, G.L. Cui, L.Q. Chen, All solid-state polymer electrolytes for high-performance lithium ion batteries, Energy Storage Mater. 5 (2016) 139–164.
[17] X. Pan, H. Sun, Z. Wang, H. Huang, Q. Chang, J. Li, J. Gao, S. Wang, H. Xu, Y. Li, W. Zhou, High Voltage Stable Polyoxalate Catholyte with Cathode Coating for All-Solid-State Li-Metal/NMC622 Batteries, Adv. Energy Mater. 10 (42) (2020) 2002416.
[18] S.F. Lou, F. Zhang, C.F. Fu, M. Chen, Y.L. Ma, G.P. Yin, J.J. Wang, Interface Issues and Challenges in All-Solid-State Batteries: Lithium, Sodium, and Beyond, Adv. Mater. 33 (2021), e2000721.
[19] S. Bag, C.T. Zhou, P.J. Kim, V.G. Pol, V. Thangadurai, LiF modified stable flexible PVDF-garnet hybrid electrolyte for high performance all-solid-state Li–S batteries, Energy Storage Mater. 24 (2020) 198–207.
[20] X. Zhang, T. Liu, S. Zhang, X. Huang, B. Xu, Y. Lin, B. Xu, L. Li, C.-W. Nan, Y. Shen, Synergistic Coupling between $Li_{6.75}La_3Zr_{1.75}Ta_{0.25}O_{12}$ and Poly(vinylidene fluoride) Induces High Ionic Conductivity, Mechanical Strength, and Thermal Stability of Solid Composite Electrolytes, J. Am. Chem. Soc. 139 (39) (2017) 13779–13785.
[21] S.-J. Tan, X.-X. Zeng, Q. Ma, X.-W. Wu, Y.-G. Guo, Recent Advancements in Polymer-Based Composite Electrolytes for Rechargeable Lithium Batteries, Electrochem. Energy Rev. 1 (2) (2018) 113–138.
[22] K.H. Wen, X. Tan, T.H. Chen, S. Chen, S.M. Zhang, Fast Li-ion transport and uniform Li-ion flux enabled by a double–layered polymer electrolyte for high performance Li metal battery, Energy Storage Mater. 32 (2020) 55–64.
[23] L.N. Dong, X.F. Zeng, J.F. Fu, L.Y. Chen, J. Zhou, S.W. Dai, L.Y. Shi, Cross-linked ionic copolymer solid electrolytes with loose Coordination-assisted lithium transport for lithium batteries, Chem. Eng. J. 423 (2021), 130209.
[24] F. He, W.J. Tang, X.Y. Zhang, L.J. Deng, J.Y. Luo, High Energy Density Solid State Lithium Metal Batteries Enabled by Sub-5 microm Solid Polymer Electrolytes, Adv. Mater. 33 (2021), e2105329.
[25] Y.R. Lu, X. Zhang, C.J. Xue, C.Z. Xin, M. Li, C.W. Nan, Y. Shen, Three-dimensional structured asymmetric electrolytes for high interface stability and fast Li-ion transport in solid-state Li-metal batteries, Mater. Today Energy 18 (2020), 100522.
[26] G.X. Wang, P.G. He, L.Z. Fan, Asymmetric Polymer Electrolyte Constructed by Metal-Organic Framework for Solid-State, Dendrite-Free Lithium Metal Battery, Adv. Funct. Mater. 31 (2020) 2007198.
[27] H. Ling, L.u. Shen, Y. Huang, J. Ma, L. Chen, X. Hao, L. Zhao, F. Kang, Y.-B. He, Integrated Structure of Cathode and Double-Layer Electrolyte for Highly Stable and Dendrite-Free All-Solid-State Li-Metal Batteries, ACS Appl Mater Interfaces 12 (51) (2020) 56995–57002.
[28] J.Q. Sun, X.M. Yao, Y.G. Li, Q.H. Zhang, C.Y. Hou, Q.W. Shi, H.Z. Wang, Facilitating Interfacial Stability Via Bilayer Heterostructure Solid Electrolyte Toward High-energy, Safe and Adaptable Lithium Batteries, Adv. Energy Mater. 2000709 (2020).
[29] W. Zhou, Z. Wang, Y. Pu, Y. Li, S. Xin, X. Li, J. Chen, J.B. Goodenough, Double-Layer Polymer Electrolyte for High-Voltage All-Solid-State Rechargeable Batteries, Adv. Mater. 31 (4) (2019) 1805574.
[30] H. Duan, M. Fan, W.-P. Chen, J.-Y. Li, P.-F. Wang, W.-P. Wang, J.-L. Shi, Y.-X. Yin, L.-J. Wan, Y.-G. Guo, Extended Electrochemical Window of Solid Electrolytes via Heterogeneous Multilayered Structure for High-Voltage Lithium Metal Batteries, Adv. Mater. 31 (12) (2019) 1807789.
[31] J.Y. Wu, L.X. Yuan, W.X. Zhang, Z. Li, X.L. Xie, Y.H. Huang, Reducing the thickness of solid-state electrolyte membranes for high-energy lithium batteries, Energy Environ. Sci. 14 (1) (2021) 12–36.
[32] X.F. Yang, K.R. Adair, X.J. Gao, X.L. Sun, Recent advances and perspectives on thin electrolytes for high-energy-density solid-state lithium batteries, Energy Environ. Sci. 14 (2) (2021) 643–671.
[33] J. Pan, Y.C. Zhang, J. Wang, Z.C. Bai, R.G. Cao, N.N. Wang, S.X. Dou, F.Q. Huang, Quasi-Double-Layer Solid Electrolyte with Adjustable Interphases Enabling High-Voltage Solid-State Batteries, Adv. Mater. (2021), e2107183.
[34] J.G. Xi, X.P. Qiu, J. Li, X.Z. Tang, W.T. Zhu, L. Chen, PVDF–PEO blends based microporous polymer electrolyte: Effect of PEO on pore configurations and ionic conductivity, J. Power Sources 157 (2006) 501–506.
[35] Z.Y. Wang, L. Shen, S.G. Deng, P. Cui, X.Y. Yao, 10 μm-Thick High-Strength Solid Polymer Electrolytes with Excellent Interface Compatibility for Flexible All-Solid-State Lithium-Metal Batteries, Adv. Mater. 33 (2021) 2100353.
[36] H.C. Gao, N.S. Grundish, Y.J. Zhao, A. Zhou, J.B. Goodenough, Formation of Stable Interphase of Polymer-in-Salt Electrolyte in All-Solid-State Lithium Batteries, Energy Mater. Adv. 2021 (2021) 1–10.
[37] J. Xi, X. Qiu, L. Chen, PVDF–PEO/ZSM-5 based composite microporous polymer electrolyte with novel pore configuration and ionic conductivity, Solid State Ionics 177 (7-8) (2006) 709–713.
[38] P. Fan, H. Liu, V. Marosz, N.T. Samuels, S.L. Suib, L. Sun, L. Liao, High Performance Composite Polymer Electrolytes for Lithium-Ion Batteries, Adv. Funct. Mater. 31 (23) (2021) 2101380.
[39] S. Xia, J. Lopez, C. Liang, Z. Zhang, Z. Bao, Y. Cui, W. Liu, High-Rate and Large-Capacity Lithium Metal Anode Enabled by Volume Conformal and Self-Healable Composite Polymer Electrolyte, Adv. Sci. 6 (2019) 1802353.
[40] W.Y. Li, H.B. Yao, K. Yan, G.Y. Zheng, Z. Liang, Y.M. Chiang, Y. Cui, The synergetic effect of lithium polysulfide and lithium nitrate to prevent lithium dendrite growth, Nat. Commun. 6 (2015) 7436.
[41] Q.-C. Liu, J.-J. Xu, S. Yuan, Z.-W. Chang, D. Xu, Y.-B. Yin, L. Li, H.-X. Zhong, Y.-S. Jiang, J.-M. Yan, X.-B. Zhang, Artificial Protection Film on Lithium Metal Anode toward Long-Cycle-Life Lithium-Oxygen Batteries, Adv. Mater. 27 (35) (2015) 5241–5247.

[42] J. Tan, J. Matz, P. Dong, J.F. Shen, M.G. Ye, A Growing Appreciation for the Role of LiF in the Solid Electrolyte Interphase, Adv. Energy Mater. 11 (2021) 2100046.
[43] R.C. Xu, X.H. Xia, S.H. Li, S.Z. Zhang, X.L. Wang, J.P. Tu, All-solid-state lithium–sulfur batteries based on a newly designed $Li_7P_{2.9}Mn_{0.1}S_{10.7}I_{0.3}$ superionic Conductor, J. Mater. Chem. 5 (2017) 6310–6317.
[44] B. Park, R. Andersson, S.G. Pate, J.C. Liu, C.P. O'Brien, G. Hernández, J. Mindemark, J.L. Schaefer, Ion Coordination and Transport in Magnesium Polymer Electrolytes Based on Polyester-co-Polycarbonate, Energy Mater. Adv. 2021 (2021) 1–14.
[45] X.B. Meng, K.C. Lau, H. Zhou, S.K. Ghosh, M. Benamara, M. Zou, Molecular Layer Deposition of Crosslinked Polymeric Lithicone for Superior Lithium Metal Anodes, Energy Mater. Adv. 2021 (2021) 1–16.